JOURNAL OF SOLID STATE CHEMISTRY 97, 1–9 (1992)

On the Structure and Some Properties of Novel Ternary Pnictides: $Na_2M_3Y_4$ (M = Sr, Eu; Y = P, As)*

WOLFGANG HÖNLE, JIANHUA LIN, MARTIN HARTWEG, AND HANS-GEORG VON SCHNERING

Max-Planck-Institut für Festkörperforschung, 7000 Stuttgart 80, Germany

Received October 2, 1991

DEDICATED TO PROFESSOR PAUL HAGENMULLER ON THE OCCASION OF HIS 70th BIRTHDAY ANNIVERSARY

Novel ternary pnictides $Na_2M_3Y_4$ (M = Sr, Eu; Y = P, As) have been prepared from binary pnictides (Na_3Y and MY) and the element Y. The compounds are isotypic to Gd_5Si_4 (Pearson code *oP* 36) as revealed by single crystal X-ray diffraction (*Pnma* (No. 62); $Na_2Sr_3P_4$: a = 735.2(2) pm, b = 1525.0(3) pm, c = 797.9(2) pm; $Na_2Eu_3P_4$: a = 729.8(2) pm, b = 1504.3(3) pm, c = 788.1(1) pm; $Na_2Eu_3As_4$: a = 745.9(2) pm, b = 1542.1(4) pm, c = 813.2(2) pm). These pnictides are Zintl phases containing M^{2+} and Na^+ cations and Y_2^{4-} dumbbells with $\bar{d}$(P–P) = 228.5 and 226.8 pm and $\bar{d}$(As–As) = 249.1 pm. The study of magnetic susceptibility and specific heat shows that $Na_2Eu_3As_4$ undergoes an antiferromagnetic phase transition at 5.38 K and a predominately ferromagnetic transition at 15.2 K.

1. Introduction

A considerable number of rare earth compounds with the general formula M_5Y_4 (M = rare earth metals; Y = P, As, Si, Ge) are known (*1–6*) to have similar structures but with different bonding between the Y atoms. The europium pnictides, Eu_5Y_4 (Y = P and As), are Zintl phases with Eu^{2+} cations and two Y^{3-} and Y_2^{4-} anions (*1, 6*). On the other hand, Gd_5Si_4, a lower symmetry version of Eu_5Y_4, contains only Si_2 dumbbells (*3*), not fulfilling Zintl's concept. According to this concept (*8*), it should be possible to have all of the Y atoms in Eu_5Y_4 as Y_2^{4-} dumbbells by replacing Eu^{2+} with alkali metal cations, etc.

In this paper, we report the synthesis and structure of $Na_2M_3Y_4$ (M = Sr, Eu; Y = P, As) as well as the magnetic properties of $Na_2Eu_3As_4$.

2. Experimental

All handling of starting materials as well as products was carried out in an argon-filled glove box ($O_2 \leq 0.5$ ppm and $H_2O \leq 0.1$ ppm) because they are both air and moisture sensitive.

* Chemistry and Structural Chemistry of Phosphides and Polyphosphides No. 57. For contribution No. 56 see J. Lin, W. Hönle, and H. G. von Schnering, *J. Less-Common Met.*, accepted for publication.

0022-4596/92 $3.00

TABLE I

CRYSTALLOGRAPHIC DATA OF $Na_2M_3Y_4$ (M = Sr, Eu; Y = P, As)

	$Na_2Sr_3P_4$	$Na_2Eu_3P_4$	$Na_2Eu_3As_4$
Molecular weight (amu)	432.74	625.76	801.55
Lattice constants (pm)	a = 735.2(2) b = 1525.0(3) c = 797.9(2)	a = 729.8(2) b = 1504.3(3) c = 788.1(1)	a = 745.9(2) b = 1542.1(4) c = 813.2(2)
Space group (No.); Z	*Pnma* (62); 4	*Pnma* (62); 4	*Pnma* (62); 4
$V(cm^3 \cdot mole^{-1})$; $d_x(g \cdot cm^{-3})$	134.7; 3.212	131.3; 4.802	140.8; 5.691
Data collection	Syntex R3 four-circle diffractometer, Mo$K\alpha$; λ = 71.073 pm, graphite monochromator; scintillation counter, ω-mode; $2\theta \leq$ 55.0°; 296 K		
Structure determination	The direct method, refinement with SHELX-76 (*10*), all atoms anisotropic, empirical absorption correction.		
$N(hkl)$; $N'(hkl)$ with $I \geq 3\sigma$	1013; 859	928; 782	1283; 1009
Variable parameters	48	50	50
$R_{(aniso)}$; $R_{w(aniso)}$	0.055; 0.048	0.041; 0.040	0.052; 0.050
Weighting	σ^{-2}	σ^{-2}	σ^{-2}

Syntheses. The corresponding mixtures (~1.5 g) of binary pnictides, Na_3Y and MY, elemental P or As in the ratio of 2 : 9 : 1 were sealed into niobium ampoules (ϕ = 15 mm and l = 80 mm). Those ampoules were heated in an evacuated quartz tube (outer container) for 2 days at 1143 K (phosphides) and 1073 K (arsenides), respectively. In the case of phosphides, a 5% excess of phosphorus and a few crystals of iodine were used in the reaction (*7*).

Properties. The crystalline materials have a metallic luster and hydrolyze in wet air, yielding smeary products, which have not been investigated further. The homogeneity of the samples was checked in each case by X-ray powder diffraction. They can be indexed on the basis of lattice parameters obtained from X-ray single crystal data. The chemical analysis of $Na_2Eu_3As_4$ gives the following results (wt%): Na (calcd 5.7; found 6.0), Eu (calcd 56.9; found 54.3), and As (calcd 37.4; found 39.7), indicating the presence of minor impurity phases, not detectable by X-ray crystallography.

Thermogravimetric studies. Thermogravimetric properties of $Na_2M_3Y_4$ (M = Sr, Eu; Y = P, As) were studied by a TGA instrument coupled with a quadrupole mass spectrometer (Netzsch STA 429; Balzers QMG 511). Weight changes and the partial pressure of particles were simultaneously detected during thermal decomposition. The sample weights are ≈50 mg; the heating rate used up to 5 K/min.

Magnetism. The magnetic susceptibility of $Na_2Eu_3As_4$ was measured with a SQUID magnetometer (SHE, VTS 805) from 4.6 to 324 K in the magnetic field of 1 kG. The measurement of specific heat of $Na_2Eu_3As_4$ was carried out on a fully automated adiabatic calorimeter in the temperature range between 1.8 and 100 K.

Structure determination. Single crystals of $Na_2M_3Y_4$ (M = Sr, Eu; Y = P, As), sealed in glass capillaries, were checked by precession photographs. The isotypic compounds crystallize orthorhombically in the space group *Pnma* (No. 62). Pertinent crystallographic data are given in Table I.

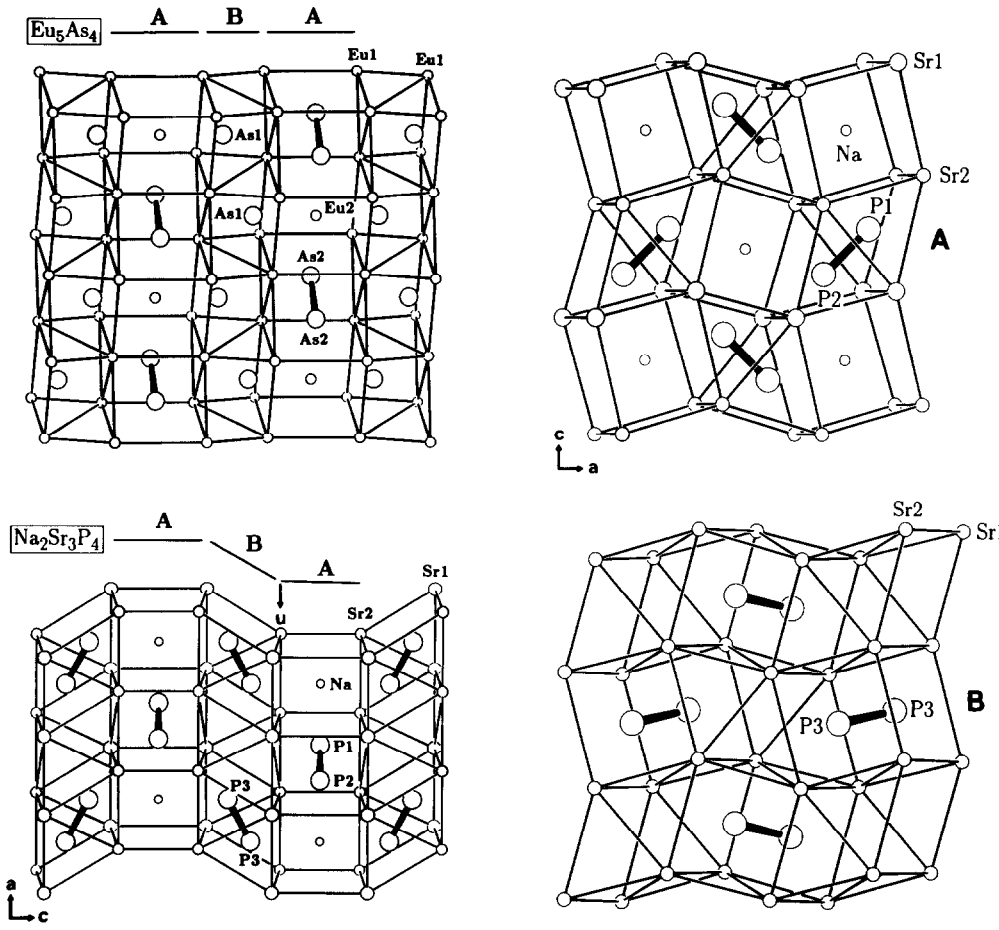

FIG. 1. Crystal structure of $Na_2Sr_3P_4$. (top left) Perspective view of Eu_5As_4 for comparison. (bottom left) Perspective view of $Na_2Sr_3P_4$. (top right) Perspective view of slab A. (bottom right) Perspective view of slab B.

The structure of $Na_2Sr_3P_4$ was determined by direct methods (*9*). Two crystallographically independent Sr positions were located from the E-map. Three phosphorus and one sodium atom were revealed from subsequent difference Fourier syntheses (*10*). From the large displacement parameter of Sr2, it became apparent that this 8*d* position was occupied statistically by Sr and Na. The site occupancy factors of both Sr2 and Na2 were refined with the constraint that their total sum is unity to 0.523(7) and 0.477, respectively. Since these values are very close to SOF = $\frac{1}{2}$, expected from the charge balance of the compound, we fixed them at $\frac{1}{2}$ in the later refinements so as to account for the composition of $Na_2Sr_3P_4$. The final refinement, with all the atoms refined anisotropically, led to a residual $R = 0.055$ and the ΔF map did not show any chemically significant feature. Our attempts to refine the structure in the lower space group $Pn2_1a$ (No. 33) did not yield significantly better results.

Using the refined parameters of $Na_2Sr_3P_4$

as a starting set, the structures of $Na_2Eu_3P_4$ and $Na_2Eu_3As_4$ were refined to give residuals of 0.047 and 0.055, respectively. In these two cases the large displacement parameters of Eu1 imply a statistical disorder as well in this position. We therefore included Na and Eu atoms in both Eu positions and constrained the sum of their occupancies at each site to unity. These refinements yielded not only significant better residual values for both structures, but also the exact composition of $Na_2Eu_3P_4$ and $Na_2Eu_3As_4$. For these three compounds, the final refined positional and displacement parameters are given in Table II. Important bond distances are presented in Table III.

3. Results and Discussion

3.1. Description of the Structure

$Na_2M_3Y_4$ (M = Sr, Eu; Y = P, As) are Zintl phases containing isolated Na^+ and M^{2+} cations and Y_2^{4-} dumbbells. Figure 1 shows the structure of $Na_2Sr_3P_4$ projected along the c-axis with $-0.32 \leq z \leq 0.32$. Two different two-dimensional slabs, namely A and B, are alternating one over the other along the b-axis. Slab A, as shown in Fig. 1, contains two types of strontium polyhedra, a Na-centered quasicube and a P_2-centered rhombic prism (*11*) formed by two neighbored trigonal prisms sharing a square face. Each quasicube connects to four of the rhombic prism by face sharing and vice versa. The P_2^{4-} dumbbells and Na atoms in slab A are located on the crystallographic mirror plans. Slab B (Fig. 1) consists of P_2-centered rhombic prisms and vacant irregular polyhedra formed by two distorted trigonal prisms. Each polyhedron shares faces with four other-type polyhedra forming the two-dimensional slab B. The observed three-dimensional structure (Fig. 1) is obtained by stacking, alternating along the b-axis, slabs A and B in such fashion that rhombic prisms and quasicubes in A are respectively connected with vacant irregular polyhedra and rhombic prisms in B.

The sodium atom at the 4*c* position is surrounded octahedrally by six phosphorus atoms of P_2^{4-} dumbbells at 2.91–3.53 Å and cubically by eight strontium atoms at 3.38–3.61 Å. The strontium atom at Sr1 position has a pentagonal bipyramidal coordination of phosphorus atoms (Fig. 2). The axial Sr1–P3 distance of 3.84 Å (thin line) is much longer than the other axial Sr1–P2 distance of 3.16 Å and hence the Sr1 coordination polyhedron could also be described as a pentagonal pyramid. The Sr2 atoms are sixfold coordinated by phosphorus atoms (Fig. 2). As clearly shown in Fig. 1, the phosphorus atoms P1 and P2 have tricapped trigonal prismatic coordination polyhedra. The capping atoms are two Na and one phosphorus atom (P1 or P2). The coordination polyhedron of phosphorus atom P3 is a bicapped trigonal prism. Na and P3 are the two capping atoms.

The structures of $Na_2Eu_3Y_4$ (Y = P, As), as mentioned already, are isomorphous with the strontium compound. The only difference is that, in the europium compounds, the Eu1 site is statistically occupied by both europium (~95%) and sodium (~5%) atoms, whereas in $Na_2Sr_3P_4$ strontium atoms alone occupy Sr1 sites. The relationship between the structures of Eu_5As_4, Sm_5Ge_4, and Gd_5Si_4 has been noted in the literature (*6*).

Eu_5As_4 crystallizes in the space group *Ccmb*, which is a minimal nonisomorphic supergroup of *Pnma*. Eu_5As_4 contains half of the As atoms as dumbbells in slab A and the other half as isolated As atoms in slab B. On the other hand, $Na_2M_3Y_4$ contains all the Y atoms as dumbbells. The difference between these two structures arises from the orientation of slab A with respect to each other. As the formal charge of two cations is reduced from +2 (Eu_5As_4) to +1 ($Na_2M_3Y_4$), slab A is forced to shift along the a-axis by a vector u so as to form the Y_2^{4-} dumbbells in slab B in between. This

TABLE II

POSITIONAL AND ANISOTROPIC DISPLACEMENT PARAMETERS FOR $Na_2M_3Y_4$ (M = Sr, Eu; Y = P, As)

Compound	Position	Site	x	y	z	Occupancy	U_{11}	U_{22}	U_{33}	U_{12}	U_{13}	U_{23}
$Na_2Sr_3P_4$	Sr1	8*d*	0.0362(1)	0.10195(6)	0.8079(1)	1	119(5)	152(5)	144(4)	32(4)	−19(4)	−10(4)
	Sr2 Na2	8*d*	0.1836(2)	0.12660(9)	0.3158(2)	½ ½	101(7)	102(7)	116(7)	−9(5)	−9(6)	4(6)
	Na	4*c*	0.3638(9)	¼	0.9916(8)	1	154(33)	344(35)	377(35)	0	22(27)	0
	P1	4*c*	0.4802(5)	¼	0.4209(5)	1	108(19)	157(17)	119(17)	0	11(15)	0
	P2	4*c*	0.2562(5)	¼	0.6169(5)	1	89(18)	136(17)	128(17)	0	29(14)	0
	P3	8*d*	0.3644(3)	0.0351(2)	0.0285(3)	1	122(13)	142(12)	125(12)	37(10)	−4(10)	−15(9)
$Na_2Eu_3P_4$	Eu1 Na1	8*d*	0.0366(1)	0.10146(4)	0.80841(6)	0.956(9) 0.044	220(6)	209(4)	169(3)	36(3)	−19(2)	−25(2)
	Eu2 Na2	8*d*	0.1837(1)	0.12642(4)	0.31435(9)	0.538(6) 0.462	210(6)	164(6)	156(4)	−6(4)	8(3)	−3(3)
	Na	4*c*	0.3648(9)	¼	0.9920(7)	1	213(46)	421(48)	353(33)	0	16(30)	0
	P1	4*c*	0.4792(6)	¼	0.4197(4)	1	197(29)	206(22)	175(16)	0	13(15)	0
	P2	4*c*	0.2560(6)	¼	0.6200(4)	1	169(28)	194(21)	201(16)	0	−12(16)	0
	P3	8*d*	0.3640(4)	0.0352(3)	0.0283(3)	1	230(20)	204(15)	174(11)	30(13)	−2(10)	−7(10)
$Na_2Eu_3As_4$	Eu1 Na1	8*d*	0.0235(1)	0.09935(5)	0.8090(1)	0.957(7) 0.043	171(4)	151(4)	161(4)	31(3)	−31(3)	−16(3)
	Eu2 Na2	8*d*	0.1789(2)	0.12681(7)	0.3200(2)	0.547(6) 0.454	171(6)	119(6)	155(6)	−7(4)	15(5)	−6(5)
	Na	4*c*	0.3566(11)	¼	0.9942(12)	1	188(41)	304(51)	282(47)	0	−54(40)	0
	As1	4*c*	0.4808(3)	¼	0.4155(3)	1	154(10)	136(10)	173(10)	0	16(8)	0
	As2	4*c*	0.2407(3)	¼	0.6285(3)	1	154(9)	113(9)	158(10)	0	10(8)	0
	As3	8*d*	0.3510(2)	0.03639(9)	0.0315(2)	1	163(7)	130(7)	158(7)	25(5)	−7(6)	−7(5)

Note. The U_{ij} are defined for $\exp\{-2\pi^2(U_{11}h^2a^{*2} + \cdots + 2U_{23}klb^*c^*)\}$ in pm^2.

TABLE III

BOND DISTANCES (pm) OF $Na_2M_3Y_4$ (M = Sr, Eu; Y = P, As)

Bond	Multiplier	$Na_2Sr_3P_4$	$Na_2Eu_3P_4$	$Na_2Eu_3As_4$
*M*1–*Y*2	1	311.0(3)	308.4(3)	317.9(2)
–*Y*3	1	313.6(3)	310.2(3)	319.1(2)
–*Y*3	1	314.2(3)	310.2(3)	320.4(2)
–*Y*1	1	315.4(3)	312.4(2)	324.3(2)
–*Y*3	1	315.6(3)	311.5(3)	321.7(2)
–*Y*2	1	315.8(3)	312.4(3)	319.0(2)
*M*2–*Y*3	1	299.5(3)	294.9(3)	301.6(2)
–*Y*3	1	299.9(3)	297.7(3)	305.6(2)
–*Y*1	1	300.0(3)	296.6(4)	304.7(2)
–*Y*3	1	301.4(3)	297.9(3)	306.3(2)
–*Y*1	1	305.7(3)	301.4(3)	307.6(2)
–*Y*2	1	311.4(3)	308.8(3)	318.0(2)
Na–*Y*1	1	290.5(7)	289.9(8)	289.8(9)
–*Y*2	1	301.8(7)	298.8(8)	303.2(9)
–*Y*2	1	307.2(7)	303.8(7)	309.7(10)
–*Y*3	2	329.0(3)	324.4(3)	330.8(2)
–*Y*1	1	353.1(7)	347.2(7)	354.9(10)
*Y*1–*Y*2	1	228.6(5)	226.8(6)	249.1(3)
–Na	1	290.5(7)	289.9(8)	289.8(9)
–*M*2	2	300.0(3)	296.6(4)	304.7(2)
–*M*2	2	305.7(3)	301.4(3)	307.6(2)
–*M*1	2	315.4(3)	312.4(2)	324.3(2)
–Na	1	353.1(7)	347.2(7)	354.9(10)
*Y*2–*Y*1	1	228.4(5)	226.8(6)	249.1(3)
–Na	1	301.8(7)	298.8(8)	303.4(9)
–Na	1	307.2(7)	303.8(7)	309.7(10)
–*M*1	2	311.0(3)	308.4(3)	317.9(2)
–*M*2	2	311.4(3)	308.8(3)	318.0(2)
–*M*1	2	315.8(3)	312.4(3)	319.2(2)
*Y*3–*Y*3	1	230.9(5)	229.3(6)	254.2(3)
–*M*2	1	299.5(3)	294.9(3)	301.6(2)
–*M*2	1	299.9(3)	297.7(3)	305.6(2)
–*M*2	1	301.4(3)	297.9(3)	306.3(2)
–*M*1	1	313.6(3)	310.2(3)	319.1(2)
–*M*1	1	314.2(3)	310.2(3)	320.4(2)
–*M*1	1	315.6(3)	311.5(3)	321.7(2)
–Na	1	329.0(3)	324.0(3)	331.0(2)

Note. Standard deviations are in parentheses.

vector u is considered to be 0 in the case of Eu_5As_4 and yields $u = 0.10$ in the compounds with dumbbells (Table IV). The formation of dumbbells Y_2 in slab B causes a shift of slab A against the other to fulfill the electronic requirements. Thus the structures of Eu_5As_4 and $Na_2M_3Y_4$ are not simple shift variants, but differ also in their crystal chemistry.

3.2. *Thermal Decomposition of* $Na_2M_3Y_4$

The thermal decomposition behavior of the three $Na_2M_3Y_4$ compounds in dynamic vacuum, studied by both thermogravimetry and simultaneous mass spectroscopy, is shown in Fig. 3. It is worth mentioning that all of these compounds initially lose sodium at temperatures of 500–550 K to form binary compounds, M_3Y_4. Similar investigations with differential thermal analyses in sealed steel ampoules show, that in the case of $Na_2Eu_3Y_4$, the emission is reversible (P compound: heating 850 K, cooling 800 K; As compound: heating 820 K, cooling 780 K). These M_3Y_4 phases, as can be seen from Fig. 2, decompose further to metal-rich binary phases by loosing Y as the temperature increases. We note, that in the case of the phosphide, the P_2^+ concentration in the gas phase is much higher than that according to a temperature-depending equilibrium $P_4/2P_2$. The emission of sodium may be explained by two oxidation processes, namely

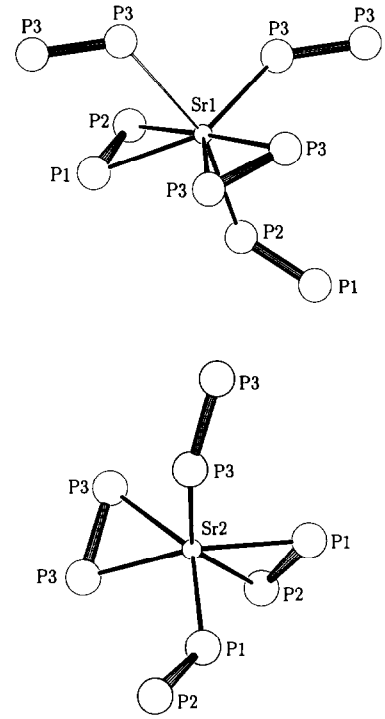

FIG. 2. Coordination polyhedron of Sr1 (top) and Sr2 (bottom).

TABLE IV

THE RELATIVE SHIFT OF x PARAMETERS FOR M_5Y_4 COMPOUNDS

	Eu_5As_4	Sm_5Ge_4	$Na_2Eu_3As_4$	Gd_5Si_4	$Na_2Sr_3P_4$	$Na_2Eu_3P_4$
Space group	*Ccmb*	*Pnma*	*Pnma*	*Pnma*	*Pnma*	*Pnma*
$x(M1)$	0.9197	0.9747	1.0235	1.0289	1.0362	1.0367
$\Delta x(M1)$	0	0.0550	0.1038	0.1092	0.1165	0.1170
$x(M2)$	0.0803	0.1205	0.1789	0.1856	0.1835	0.1837
$\Delta x(M2)$	0	0.0402	0.0986	0.1053	0.1032	0.1034
Shift vector u	0	0.0048	0.101	0.107	0.110	0.110
Shortest Y–Y Distance (Å)	4.33	3.71	2.54	2.48	2.31	2.29

$2Eu^{2+} \rightarrow 2Eu^{3+} + 2e^-$ or the linkage of two Y_2^{4-} dumbbells, leading to $2Y_2^{4-} \rightarrow Y_4^{6-} + 2e^-$. The Y_4^{6-} unit is part of the structure of Eu_3Y_4 which is found in the TG after the complete emission of Na. At higher temperatures we found the well-known decomposition behavior of the europium phosphides and arsenides, respectively, according to $Eu_3As_4 \rightarrow EuAs \rightarrow Eu_{11}As_{10} \rightarrow Eu_5As_4$.

3.3. The Magnetic Properties of $Na_2Eu_3As_4$

Figure 4 shows the temperature variations of the magnetic susceptibility χ_m of $Na_2Eu_3As_4$, and the effective magnetic moment, μ_{eff}, calculated from the Curie law. The effective magnetic moment, μ_{eff} ($Na_2Eu_3As_4$), at 298 K is 7.1 B.M. per Eu atom, indicating that all europium atoms are present as Eu^{2+}. The magnetic susceptibility follows the Curie–Weiss law in the temperature region $40 \leq T(K) \leq 324$ with $\theta = 11.3$ K. Below 40 K the magnetic susceptibility deviates from the Curie–Weiss law with a major anomaly at about 6 K and a shoulder at about 15 K (Fig. 4).

The magnetic specific heat, C_p^{mag}, of $Na_2Eu_3As_4$, obtained by substracting the lattice contribution (*11*) from the measured specific heat C_p, is given in Fig. 4 (top). The unambiguous observation of a sharp and nearly symmetrical transition at 5.38 K and a λ-shaped transition at 15.2 K is consistent with the magnetic susceptibility data. The magnetic entropy $S_{mag} = 49.3$ J mol^{-1} K^{-1} given by $\int_0^\infty (C_p^{mag}(T)/T)\,dT$ is about 5% less than the theoretical value of 3 Rln($2S + 1$) = 51.9 J mol^{-1} K^{-1} for a spin system with $S = 7/2$.

By considering the large positive value of the Curie–Weiss constant, the first λ-shaped transition at 15.2 K could be a transition into a predominately ferromagnetic intermediate phase. Moreover the large entropy changes ($\Delta S_{mag} = 22.0$ J mol^{-1} K^{-1}) between the two critical points (5.38–15.2 K) is probably an indication of the incommensurate nature of this intermediate phase. The other very sharp transition at 5.38 K, which is accompanied by a sharp decrease of magnetic susceptibility, corresponds to the transition into an antiferromagnetic state.

As mentioned already, the arsenic atoms in $Na_2Eu_3As_4$ are located at the centers of trigonal prisms of europium atoms. There are, on the average, two kinds of Eu–As–Eu angles, i.e., 80° and 130°. It is commonly known that a straight metal–anion–metal arrangement tends to have an antiferromagnetic coupling, whereas a rectangular arrangement preferably leads to a ferromagnetic coupling. Based on the structure, we could infer that the observed magnetic transitions of the $Na_2Eu_3As_4$ compound arise from the competition of ferromagnetic and antiferromagnetic orderings. The ferromagnetic coupling could be

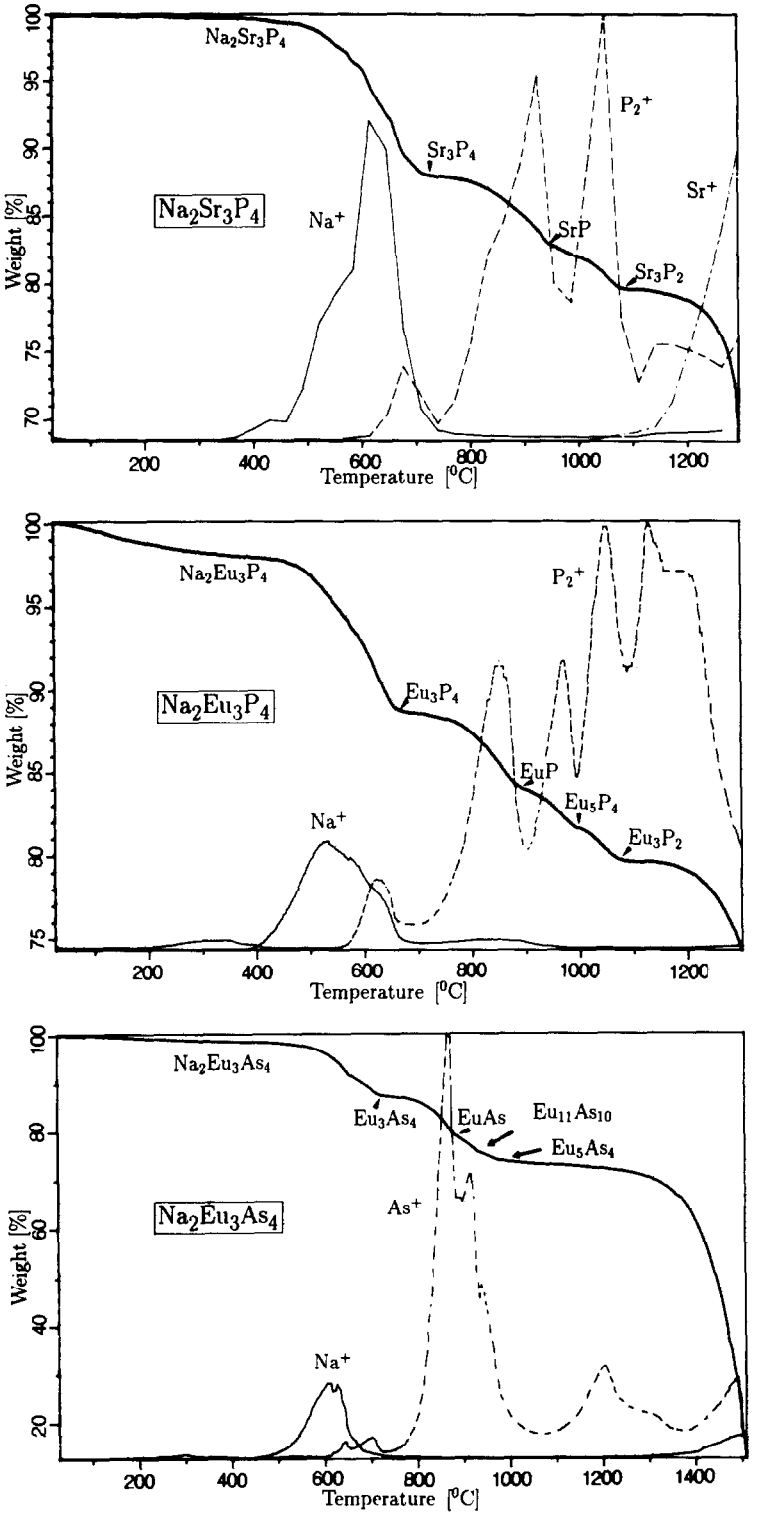

FIG. 3. Thermal decomposition behavior of $Na_2Sr_3P_4$ (top), $Na_2Eu_3P_4$ (center), and $Na_2Eu_3As_4$ (bottom) in dynamic vacuum. The thermogravimetric curve (TG) with the appearing phases is shown as thick solid line. Mass spectra of Na^+ (—) and P_2^+/As^+ (---).

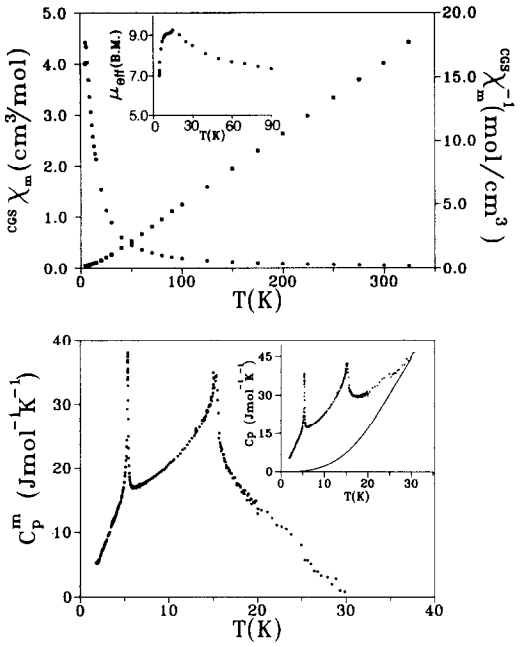

FIG. 4. (top) Temperature variation of magnetic susceptibility (●), reciprocal magnetic susceptibility (■), and effective magnetic moment (insert) of $Na_2Eu_3As_4$. (bottom) Temperature variation of magnetic specific heat (c_p^{mag}) of $Na_2Eu_3As_4$. (insert) Specific heat (c_p) and lattice contribution (solid) versus temperature.

expected to be larger than the antiferromagnetic coupling and this is in fact visualized from the large positive Curie–Weiss constant. This is why the compound undergoes a predominately ferromagnetic ordering first at 15.2 K and a final antiferromagnetic ordering at lower temperature (5.38 K). The magnetic behavior of $Na_2Eu_3As_4$, in some aspects, is similar to that of $EuAs_3$ (*13–15*), which has been proved to have an antiferromagnetic phase below 10.26 K and an incommensurate phase between 10.26 and 11.30 K.

Acknowledgments

We thank Dr. K. Peters for the single crystal X-ray data collection, Professor E. Gmelin for specific heat measurement and helpful discussions, Mr. M. Gehrke for magnetic susceptibility measurement, Ing. grad. Chr. Mensing and Mrs. S. Prill for thermogravimetric studies, and Dr. K. Vidysagar for helpful discussions.

References

1. H. G. VON SCHNERING AND W. HÖNLE, *Chem. Rev.* **88,** 243 (1988).
2. S. ONO, F. L. HUI, J. G. DESPAULT, L. D. CALVERT, AND J. B. TAYLOR, *J. Less-Common. Met.* **25,** 287 (1971).
3. J. IGLESIAS AND H. STEINFINK, *J. Less-Common Met.* **26,** 45 (1972).
4. G. S. SMITH, Q. JOHNSON, AND A. G. THARP, *Acta Crystallogr.* **22,** 269 (1967).
5. G. S. SMITH, A. G. THARP, AND Q. JOHNSON, *Nature (London)* **210,** 1148 (1966).
6. Y. WANG, L. D. CALVERT, E. J. GABE, AND J. B. TAYLOR, *Acta Crystallogr. B* **34,** 1962 (1978).
7. H. SCHÄFER AND M. Z. TRENKEL, *Z. Anorg. Allg. Chem.* **391,** 11 (1972).
8. R. NESPER, *Prog. Solid State Chem.* **20,** 1 (1990).
9. G. M. SHELDRICK, "SHELXS-86," Institut für Anorganische Chemie der Universität, Göttingen, FRG.
10. G. M. SHELDRICK, "SHELX-76," University of Cambridge, 1976.
11. H. NYMAN, *J. Solid State Chem.* **17,** 75 (1976).
12. The lattice contribution of specific heat has been estimated by the Debye function with a temperature-dependent effective Debye temperature. The Debye temperature, obtained in this way, varies from $\Theta_D = 300$ K to $\Theta_D = 210$ K as the temperature decreases from 100 to 30 K. Below 20 K the Debye temperature is fixed to 205 K to calculate the lattice contribution in this range. The estimated deviation of the magnetic entropy, arising from fixing the Debye temperature, has been calculated by varying the Debye temperature with $\delta\Theta_D = \pm 10$ K and was found to be $\delta S = \pm 2.0$ J mol^{-1} K^{-1} which is about 5% of the total magnetic entropy. The magnetic specific heat below 1.8 K was estimated by a linear extrapolation.
13. W. BAUHOFER, E. GMELIN, M. MÖLLENDORF, R. NESPER, AND H. G. VON SCHNERING, *J. Phys. C.* **18,** 3017 (1985).
14. T. CHATTOPADHYAY, P. J. BROWN, P. THALHEIMER, AND H. G. VON SCHNERING, *Phys. Rev. Lett.* **57,** 372 (1986).
15. T. CHATTOPADHYAY, H. G. VON SCHNERING, AND P. J. BROWN, *J. Magn. Magn. Mater.* **28,** 247 (1982).